1-1-2003

Intelligent Strain Sensing on a Smart Composite Wing using Extrinsic Fabry-Perot Interferometric Sensors and Neural Networks

Kakkattukuzhy M. Isaac
Missouri University of Science and Technology, isaac@mst.edu

Donald C. Wunsch
Missouri University of Science and Technology, dwunsch@mst.edu

Steve Eugene Watkins
Missouri University of Science and Technology, watkins@mst.edu

Rohit Dua
Missouri University of Science and Technology, rdua@mst.edu

et. al. For a complete list of authors, see http://scholarsmine.mst.edu/ele_comeng_facwork/1691

Recommended Citation

Intelligent Strain Sensing on a Smart Composite Wing using Extrinsic Fabry-Perot Interferometric Sensors and Neural Networks.

Rohit Dua[1], Vicki Eller[2], Kakkattukuzhy M. Isaac [3], Steve E. Watkins[2], and Donald C. Wunsch[1]

[1]Applied Computational Intelligence Laboratory
[2]Applied Optics Laboratory
Department of Electrical and Computer Engineering
[3]Department of Mechanical and Aerospace Engineering
University of Missouri-Rolla
Rolla, MO-65409, USA

Abstract – Strain prediction at various locations on a smart composite wing can provide useful information on its aerodynamic condition. The smart wing consisted of a glass/epoxy composite beam with three Extrinsic Fabry-Perot Interferometric (EFPI) sensors mounted at three different locations near the wing root. Strain acting on the three sensors at different air speeds and angles-of-attack were experimentally obtained in a closed circuit wind tunnel under normal conditions of operation. A function mapping the angle of attack and air speed to the strains on the three sensors was simulated using feed-forward neural networks trained using back-propagation training algorithm. This mapping provides a method to predict stall condition by comparing the strain available in real time and the predicted strain by the trained neural network.

I INTRODUCTION

Advanced composite materials are being used in substantial amounts for the development and construction of advanced aerospace structures [1] that provides the structures with clear advantages of long life, high strength-to-weight ratio, and flexible design. A built-in Health Monitoring System (HMS) can monitor structural condition, and react to any changes in environment, resulting in a smart structure [2-3]. Research in HMS development for efficient smart structures has improved capability in data interpretation or control functions [3-6]. The choice of an optical sensor system, an important component of a HMS, has proven to be an effective choice owing to the number of advantages over non-optical sensors including little perturbation to the host structure, immunity to electromagnetic interference and the ability to form multiplexed networks for complex measurements [2]. Advances in fiber optic sensing technology are reducing the weight, required power, and the cost. Fiber optic sensor based HMS have been used for monitoring structural integrity [7-8], vibration control [9], and damage assessment using modal analysis [10].

Artificial Neural Networks (ANN) are being used extensively as an efficient processing system due to their capabilities in pattern recognition, classification and function approximation [4-6, 10-11]. The integration of optical sensor system and ANNs has enhanced the applications of fiber-reinforced composite components into aerospace systems. Research has been carried out on the development of a smart helicopter rotor model using neural networks [12]. Neural networks are being extensively used in many aerospace applications including auto-pilots, flight path simulations, control systems, component simulations and fault detection [13].

Prediction of aerodynamic parameters under varying load conditions on an aircraft wing would provide useful information on the working condition of the wing. One such parameter is the strain levels acting at various points on the wing. The mathematical modeling of strain levels using known parameters such as angle-of-attack and wind speed is highly complex and not feasible. Complication factors are unpredictable wing stall, conditions on the wing surface, and changes in environmental conditions such as icing, rain, dirt; wind turbulence and shear. These varying input parameters cannot be accurately modeled using mathematical equations. The use of predictive and adaptive tools, like ANNs, that learn from data obtained from sensors can model to high accuracy. The data from the sensors incorporate the unpredictable conditions. The fusion of efficient fiber optic sensor technology and neural networks provides a possible solution to modeling the strains acting on different points on the wing and lead to an improvement in flight safety, and maintenance.

Prior research has been carried out on the modeling of strain acting on the sensor attached on the wing root using neural networks [14]. This paper deals with an extension of the approach. Here, a more complex and aerodynamic wing was used and multiple sensors were distributed along the length of wing. The next section gives a brief overview on fiber optic sensors used in this test and its support system. The third section deals with the experimentation carried out to obtain the strains from the sensors under varying parameters of angle-of-attack and speed. The fourth section gives two types of neural network implementations for the sensors. The final section gives the conclusions and insight into future work to be carried out.

II FIBER OPTIC SENSORS

Common fiber optic sensors are based on interferometric and attenuation effects. Apart from being immune to electromagnetic interference, non-conductive to electrical sources, capable of wide temperature operation, and safe in inflammable or explosive environment, fiber optic sensors can be embedded into composite structures, have high bandwidth, may be multiplexed, and are capable of serving not only as sensors but also mediums to relay their information [2,8,15]. Interferometric sensors are more sensitive and are localized in sensing compared to attenuation systems. Fabry-Perot sensors have added advantages over other interferometric types. They have no reference arm requirement as in Michelson or Mach-Zehnder sensor and are single ended [2].

This research uses the extrinsic Fabry-Perot interferometric (EFPI) sensor, Figure 1, to sense the strain levels. EFPI sensors have short gauge length and consequently are used for point strain measurement.
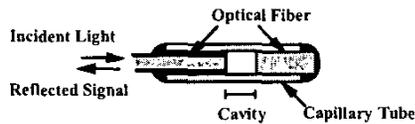

Figure 1: Extrinsic Fabry-Perot Interferometric (EFPI). The optical output is the reflected signal formed by the interference of multiple reflections from the glass-air interfaces of the cavity.

The sensor instrumentation is shown in Figure 2. The sensor and instrumentation used in this study were manufactured by Luna Innovations, Inc, and were capable of absolute strain measurements. Also, multiple EFPI sensors can be multiplexed at a scanning rate of one-Hertz per sensor channel.
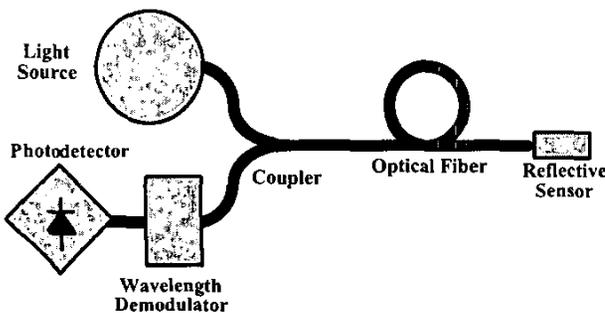

Figure 2: Schematic diagram of the fiber-optic support system It consists of a light emitting diode (LED), an optical isolator, a 2×1 coupler, and a detection apparatus.

An LED source provides the input light beam into the single mode fiber. A coupler and wavelength demodulator branches the reflected interference fringes to a detector. The interference response at several wavelengths can determine the absolute cavity displacement and hence the absolute strain.

III EXPERIMENTATION

A fiber-reinforced composite wing with an aluminum frame was manufactured in the Composite Fabrication Laboratory at the University of Missouri-Rolla. The wing has a NACA 0012 airfoil section. The chord length is 10 cms and the span is 50.8 cm. The wing has of two spars made of stainless steel rods and aluminum ribs spaced ~100 cm apart. The aluminium ribs were first machined in the shape of the airfoil section and the steel rods were inserted in holes drilled in the ribs, providing a skeleton for the wing. Styrofoam blocks inserted between the spars were then shaped to form the airfoil section, accomplished by cutting the styrofoam using a thin heated wire. Fiberglass cloth was used form the skin. After wrapping with the cloth, resin was applied to provide the final composite wing. The wing surface was sanded to a fine finish, taking precautions to maintain the airfoil cross section shape. The finished wing was then examined for structural integrity and geometrical accuracy. The fiber optic sensors were mounted in grooves cut in the styrofoam prior to covering with fiberglass cloth. The optical fibers from the sensors were placed in channels formed on the wing prior to installing the cloth covering. After installing the cloth, applying the resin and sanding, the sensors and the fibers were hardly noticeable and did not cause any surface irregularity. The wing had a top view as shown in Figure 3, showing the aerodynamic wind direction.
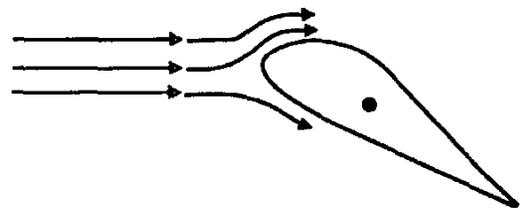

Figure 3: Top-view of the Composite Wing used in Experimentation. Aerodynamic forces are created by the pressure and shear stress distributions leading to a strain field over a wing surface.

Key strain points can be monitored using EFPI sensors under different operating conditions. Monitoring the strain at pre-decided locations on the wing surface, can provide useful information in modeling wing stall. Three EFPI sensors were strategically placed on the upper surface at the wing root as shown in Figure 4.
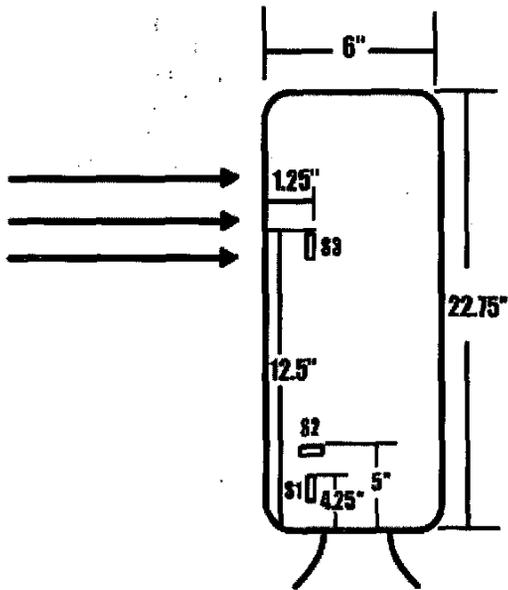
Figure 4: Sensor placement on the surface of the wing. The arrows show the direction of wind-flow.

The experiments were conducted in a closed circuit wind tunnel. The wind tunnel test section measured 120 × 76 cm. The air speed was measured using a pitot-static tube and a digital dynamic pressure sensor. The strain readings were recorded using the attached sensors and associated instrumentation. The only parameters that were varied were the air-speed and angle-of-attack. The variation in the angle-of-attack was measured as shown in Figure 5.
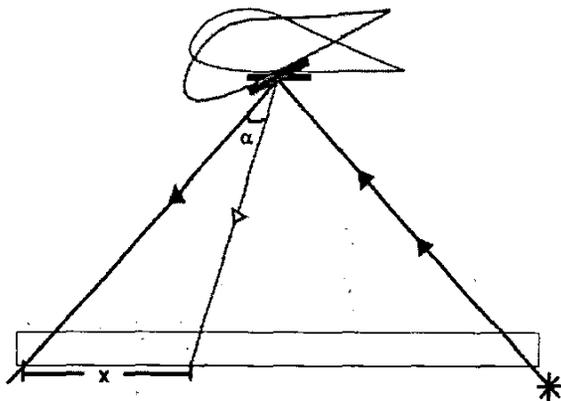

Figure 5: Setup for Measuring the Angle-of-Attack. Fixed increments of 1 cm in horizontal scale bring about a change in angle-of-attack. A mirror was mounted at the wing root. A laser beam is bounced off the mirror to a ruler. Rotation in the wing angle (∝) brings about a horizontal shift in the beam (x).

The dynamic pressure was varied between 0 Pa and 460 Pa for a particular horizontal increment in angle-of-attack. The variation in the angle-of-attack (∝) was brought about by the variation in the horizontal scale in increments of 1cm between -4 cm to +11 cm (for ∝ between -1.627° and +4.31°). Sampled versions of the time-based strains were stored at a sampling rate of 3 Hz as shown in Figure.6. A total of 103 test samples were recorded, for each sensor, by the combination of different air speeds and angle-of-attacks. The next section deals with the modeling of these strains to the input parameters of air speed and angle-of-attack.
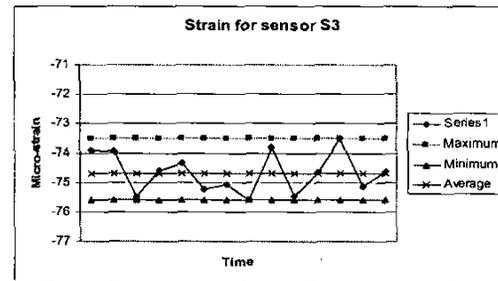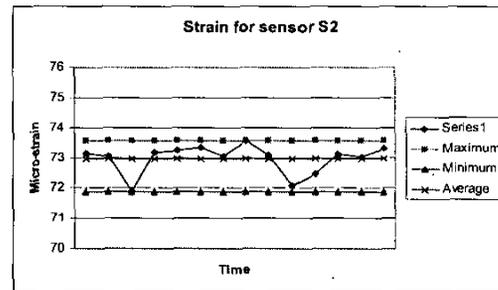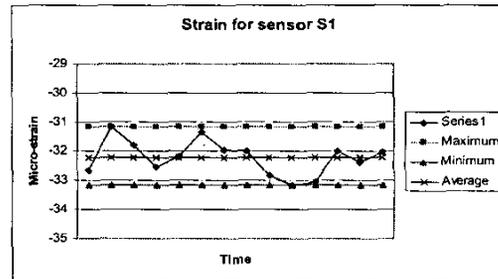

Figure 6: Sampled versions of strains from the three sensors. Note the small range over which the strain varies. This range may vary depending on the sampling time. A set of neural networks was trained on maximum and minimum values of strain and another set was trained on average strain values.

IV NEURAL NETWORK IMPLEMENTATION

The networks were trained on two types of sensor data. Note from figure 6, the sensor output varies over a range of

values. The results of training and simulation of the networks on the maximum and minimum, and average strain values are compared.

A. Training on Minimum and Maximum Strain Values

A total of three neural networks were implemented, one for each sensor. The networks varied in the architecture, owing to the difference in their placement, resulting in a different mapping function. For all the three networks, the input and output data was normalized and scaled between -1 and 1. A 2,38,2 ANN for sensor 'S1', 2,42,2 ANN for sensor 'S2', and 2,42,2 ANN for sensor 'S3' were used to train and simulate the three sensors. The output layer has 2 neurons, because the network was trained to the minimum and maximum strain values. The transfer functions of the input and output layers are 'TANSIG' and 'PURELIN' respectively. The networks were trained using Levenberg-Marquardt backpropagation training algorithm to the desired mean square error of 1e-5. For all the three networks, 94 vectors were used for training and 9 for testing the trained network.

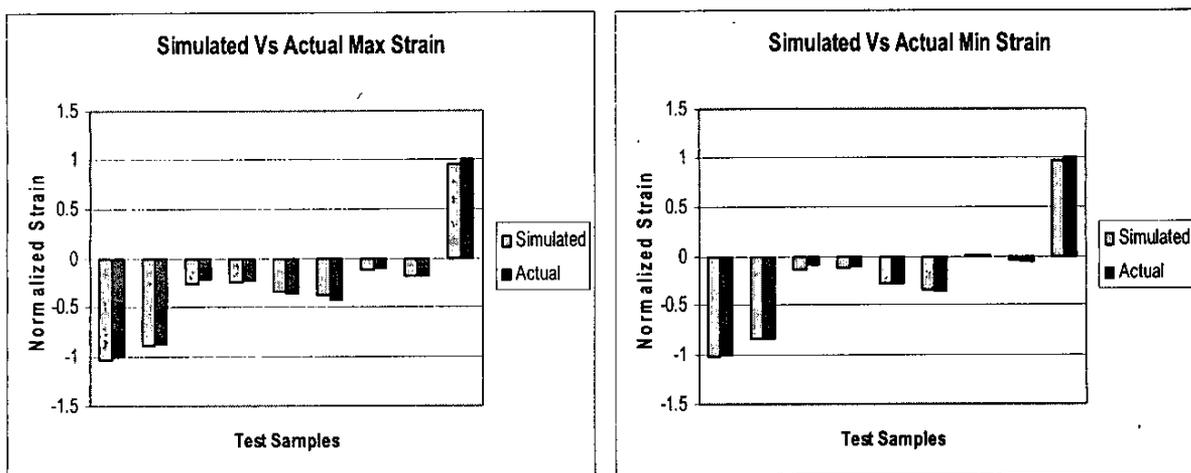Figures 7, 8 and 9 show the simulation results for the sensor 'S1', 'S2' and 'S3' respectively.

Figure 7: Simulation results for maximum and minimum strain for sensor 'S1'. The maximum absolute error for maximum and minimum strain is 15% and 60% respectively.
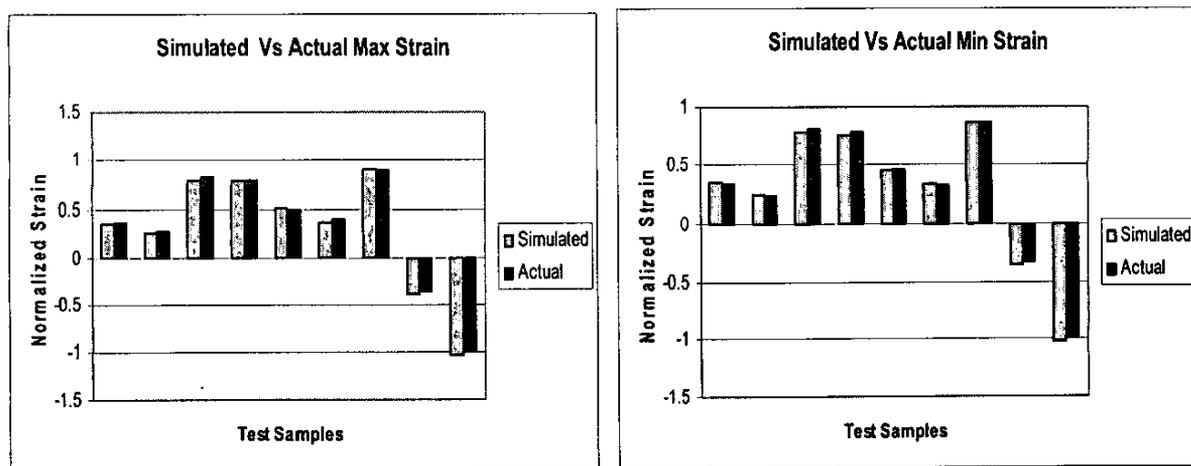

Figure 8: Simulation results for maximum and minimum strain for sensor 'S2'. The maximum absolute error for maximum and minimum strain is 9.7% and 8.3% respectively.
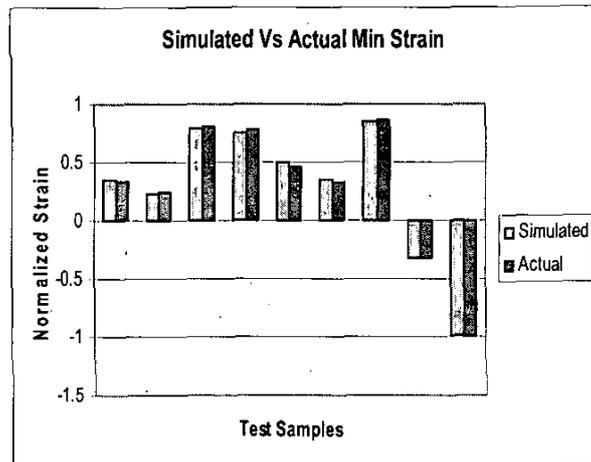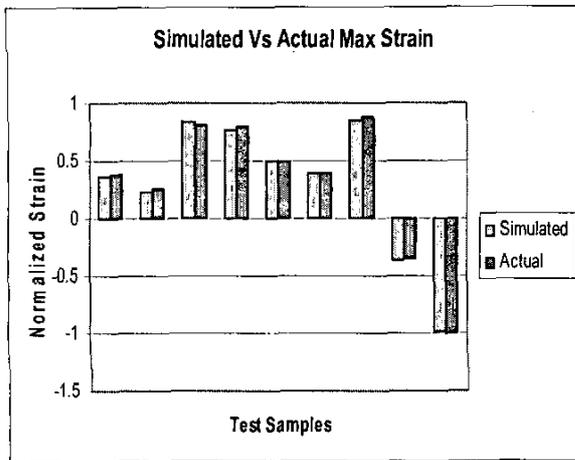
Figure 9: Simulation results for maximum and minimum strain for sensor 'S3'. The maximum absolute error for maximum and minimum strain is 15.8% and 9.27% respectively.

B. Training on Average Strain Value.

A total of three neural networks were implemented, one for each sensor. The networks varied in the architecture, owing to the difference in their placement, resulting in a different mapping function. For all the three networks, the input and output data was normalized and scaled between -1 and 1. A 2,30,1 ANN for sensor 'S1', 2,30,1 ANN for sensor 'S2', and 2,36,1 ANN for sensor 'S3' were used to train and simulate the three sensors. The output layer has 1 neuron, because the network was trained to the average value. The transfer functions of the input and output layers are 'TANSIG' and 'PURELIN' respectively. The networks were trained using Levenberg-Marquardt backpropagation training algorithm to the desired mean square error of 1e-5. For all the three networks, 94 vectors were used for training and 9 for testing the trained network.

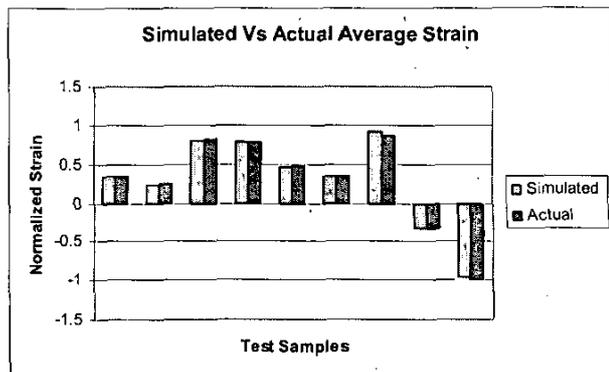Figures 10, 11 and 12 show the simulation results for the sensor 'S1', 'S2' and 'S3' respectively.
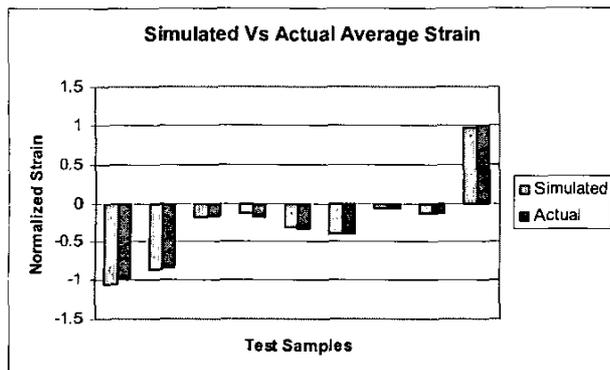

Figure 10: Simulation results for average strain for sensor 'S1'. The maximum absolute error for strain is 38.1% respectively.

Figure 11: Simulation results for average strain for sensor 'S2'. The maximum absolute error for strain is 6.82% respectively.

Figure 12: Simulation results for average strain for sensor 'S3'. The maximum absolute error for strain is 6.34% respectively
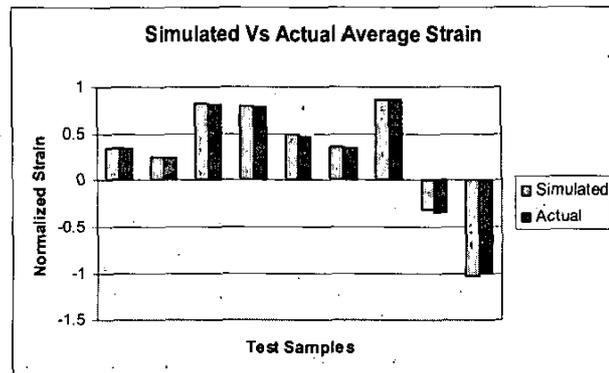
2671

V CONCLUSION AND FUTURE WORK.

The strains at the three different locations, on the surface of a composite wing, were modeled to the varying parameters of air speed and angle-of-attack. Senor locations on the wing were chosen near the wing root where the strain is largest. The result obtained provides a strong foundation to the development of a system that will help in the prediction of stall and thereby avoid serious consequences arising from it. Future work will look into simulating stall condition and testing the trained networks to predict the stall. Online training of the networks to time varying input parameters will be investigated. Improvements in the measurement of angle-of-attack and airspeed could improve the system accuracy. Also, optimal sensor locations will be found, using techniques like Finite Element Analysis (FEA), to maximize performance; as each strain point is modeled using a different architecture of the neural network.

VI REFERENCES

[1]. J. Edmonds, and G. A. Hickman , "Damage Detection and Identification in Composite Aircraft Components," *IEEE Aerospace Conference Proceedings*, 2000, Vol. 6 , 2000, pp. 73 -77

[2]. E. Udd, "Fiber Optic Smart Structures," *Proceedings of the IEEE*, 84 (6), 884-894 (1996)

[3]. W. B. Spillman Jr., "Sensing and Processing for Smart Structures," *Proceedings of the IEEE*, 84 (1), 68-77 (1996).

[4]. V. Rao, R. Damle, "Identification and Control of Smart Structures using Neural Networks," *Proceedings of the 33rd IEEE Conference on Decision and Control*, 1, 91-96 (1994)

[5]. P. Tsou, and M. H. H. Shen, "Structural Damage Detection and Identification Using Neural Networks," *AIAA Journal*, 32 (1), 176-183 (1994).

[6]. R. Ceravolo, A. De Stefano, and D. Sabia, "Hierarchical use of Neural Techniques is Structural Damage Recognition," *Smart Materials and Structures*, 4, 270-280 (1995).

[7]. K. A. Murphy, M. F. Gunther, A. M. Vengsarkar and R. O. Claus, "Fabry-Perot Fiber Optic Sensors in Full-Scale Fatigue Testing on an F-15 Aircraft," *Applied Optics*, 31, pp. 431-433 (1992).

[8]. K. F. Hale, "An Optical-fiber Fatigue Crack-detection and Monitoring System," *Smart Materials and Structures*, 2, 156-161 (1992).

[9]. S. M. Yang, and J. A Jeng, "Vibration Control of a Composite Plate with Embedded Optical Sensor and Piezoelectric Actuator," *Journal of Intelligent Material Systems and Structure*, 8, 393-9 (1997).

[10]. S. E. Watkins, G. W. Sanders, F. Akhavan, and K. Chandrashekhara, "Modal Analysis using Fiber Optic Sensors and Neural Networks for Prediction of Composite Beam Delamination," *Smart Materials and Structures*, 11, 489-495 (2002).

[11]. R. Dua, S. E. Watkins, D. C. Wunsch, K. Chandrashekhara, and F. Akhavan, "Detection and Classification of Impact-Induced Damage in Composite Plates using Neural Networks," *INNS-IEEE International Joint Conference on Neural Networks*, (Mount Royal, NJ: International Neural Network Society) (*Washington DC, July 2001*) p 51.

[12]. R. Ganguli, I. Chopra, and D. J. Haas, "Helicopter Rotor System Fault Detection using Physics-Based Model and Neural Networks," *AIAA Journal*, 36, 1078-1086 (1998).

[13]. M.T. Hagan, H.B. Demuth, M. Beale, Neural Network Design (PWS Publishing Company, Boston), 1996

[14]. A. Lunia, K. M. Isaac, K. Chandrashekhara, and S. E. Watkins, "Aerodynamic Testing of a Smart Composite Wing using Fiber–Optic Strain Sensing and Neural Networks," *Smart Materials and Structures*, 9, 767-773 (2000).

[15]. M. R. Sayeh, R. Viswanathan, and S.K. Dhali, "Neural Networks for Smart Structures with Fiber Optic Sensors", *Proceedings of OE/Midwest: 1990, Proc. SPIE. 1396, 417-429 (1990).*